Investigation of Immune-related Makers Associated with Tumor-infiltrating T Cells in Ovarian Cancer

Haihong Liao
Huzhou Central Hospital
Shuwen Han
Huzhou Central Hospital
Yuefen Pan
Huzhou Central Hospital
Jiamin Xu
Huzhou University
Quan Qi
Huzhou Central Hospital
Yizhen Jiang
Huzhou Central Hospital
Xi Yang (yangxi0601@hotmail.com)
Huzhou Central Hospital https://orcid.org/0000-0003-2382-0282

Research

Keywords: Ovarian cancer, tumor-infiltrating T cells, prognosis

Posted Date: August 6th, 2020

DOI: https://doi.org/10.21203/rs.3.rs-53352/v1

Abstract

Background: Tumor-infiltrating T cells in the tumor microenvironment are the biological basis of immunotherapy and promising predictors of cancer prognosis.

Aim: The aim of this study was to investigate immune-related RNAs associated with tumor-infiltrating T cells in ovarian cancer (OV).

Methods: The gene expression data of patients with OV were downloaded from The Cancer Genome Atlas (TCGA) database. The immune and stromal scores were calculated and the differentially expressed mRNAs (DEGs) were screened. The abundance of six types of infiltrating immune cells was investigated, and the immune-related DEGs associated with tumor-infiltrating $CD4^+$ and $CD8^+$ T cells were explored by correlation analyses. Subsequently, multiple analyses, i.e., protein-protein interaction (PPI) network analysis, competing endogenous RNA (ceRNA; lncRNA-miRNA-target) network analysis, and small-molecule target network analysis, were performed.

Results: In total, 37 and 49 immune-related DEGs of $CD4^+$ and $CD8^+$ T cells were screened, respectively. PPI network results showed that granzyme B (GZMB) was a hub node in the two PPI networks constructed by immune-related DEGs of $CD4^+$ and $CD8^+$ T cells. Moreover, the ceRNA chr22-38_28785274-29006793.1/has-miR-1249-5p/CD3E was obtained from the two constructed ceRNA networks related to $CD4^+$ and $CD8^+$ T cells. Survival analysis revealed that key immune-related DEGs of $CD4^+$ and $CD8^+$ T cells, such as GZMB and CD3E, were positively correlated with patient prognosis.

Conclusion: GZMB and ceRNAs, such as chr22-38_28785274-29006793.1/has-miR-1249-5p/CD3E, may mediate the role of tumor-infiltrating T cells in OV. GZMB and CD3E may be used as promising T cell-related biomarkers with prognostic value in OV.

Highlights

1. Tumor-infiltrating T cells may influence patient prognosis by regulating GZMB.
2. chr22-38_28785274-29006793.1/has-miR-1249-5p/CD3E may mediate the role of tumor-infiltrating T cells in OV.
3. GZMB and CD3E may serve as promising prognostic biomarkers for OV.

Introduction

Ovarian cancer (OV) is a common lethal gynecological malignancy with a rising mortality rates (1–3). The prognosis of patients with OV is poor due to lack of early symptoms and the high proportion of patients with advanced stage OV (> 60%), which have a five-year survival rate of just 40% (4, 5). Therefore, the exploration of key mechanisms associated with cancer prognosis will facilitate the design of effective therapeutics to improve the clinical outcomes of OV.

Cancer immunotherapy has recently achieved remarkable success in the treatment of late-stage tumors (6, 7) and in elucidating the potential role of the tumor immune microenvironment in tumor progression (8). Accumulating evidence has revealed that OV is an immunogenic disease recognized by the host immune system (9). Tumor-infiltrating lymphocytes (TILs), which indicate an ongoing host immune response against cancer cells, exist in the tumor microenvironment and impact the prognostic value of patient-reported outcomes in various cancer entities (10–13). TILs (e.g., T-cells, macrophages, B-cells, or natural killer cells) are types of white blood cells capable to infiltrate solid tumors. Cytotoxic $CD8^+$ T cells are shown to play a key role in the direct recognition and elimination of tumor cells, and can be recruited and activated by non-cytotoxic $CD4^+$ T cells to promote anti-tumor response. Tumor-infiltrating T cells, especially $CD4^+$ and $CD8^+$ T cells, are considered as powerful prognostic indicators of clinical outcomes in patients with OV (14, 15).

In addition, gene expression in tumor tissues is found to be significantly affected by the tumor microenvironment, and subsequently influences the prognosis of patients (16). Immune and stromal cells are important components of the tumor microenvironment that have exhibited diagnostic and prognostic values in tumors (17, 18). Increasing studies have revealed tumor microenvironment-associated biomarkers with prognostic value in various cancers on the basis of gene expression data of immune and/or stromal cells (19, 20). However, the immune-related markers associated with tumor-infiltrating T cells in OV have not been fully explored.

In the present study, we downloaded the gene expression data of patients with OV from The Cancer Genome Atlas (TCGA) database, and then analyzed the differentially expressed mRNAs (DEGs) on the basis of the immune and stromal scores, which were calculated by the Estimation of STromal and Immune cells in MAlignant Tumours using Expression data (ESTIMATE) algorithm. The ESTIMATE algorithm could provide scores for estimating the levels of stromal cells and infiltrating immune cells in tumor tissues as well as tumor purity (21). Subsequently, the immune-related DEGs associated with tumor-infiltrating T cells were screened by correlation analysis, followed by protein-protein interaction (PPI) network analysis, competing endogenous RNA (ceRNA; lncRNA-miRNA-target) network analysis, small-molecule target network analysis, and survival analysis. The flow chart of the comprehensive bioinformatic analysis is shown in Supplemental Fig. 1. We aimed to analyze the immune-related RNAs associated with tumor-infiltrating T cells in OV. The findings of our study will provide theoretical guidance for studying the molecular mechanism of immune escape in OV and exploring the promising T cell immune-related biomarkers for OV therapy and prognosis.

Data And Methods

Data source

This study used data available in the public domain. The gene expression data and clinical data of patients with OV (version07-20-2019) were downloaded from the TCGA database (https://xenabrowser.net/). A total of 373 tumor samples were included.

Calculation of immune and stromal scores

In accordance with the annotation information of the platform, the empty probes were removed, and the mean value of multiple probes mapped to the same gene was considered as the mRNA expression level. Immune and stromal scores were then calculated by means of the ESTIMATE algorithm (version 1.0.13) (21) in R package.

DEGs screening

Based on the median value, all samples were assigned as high and low immune score groups as well as high and low stromal score groups. The DEGs in high vs low immune score as well as in high vs low stromal score groups were respectively screened using the limma package (version 3.10.3, http://www.bioconductor.org/packages/2.9/bioc/html/limma.html) (22) in R package. Using the method of Benjamini-Hochberg (23), the adjusted *p*-value was obtained. The cutoff criteria for DEGs were adjusted to $p < 0.05$ and |log fold change (FC)|□0.585. The volcano plots for DEGs were visualized using ggplot2 (version: 3.2.1). The intersection DEGs were then obtained by a VENN analysis.

Functional enrichment analysis

Functional enrichment analyses for intersection DEGs, including Gene Ontology (GO)-biological process (BP) (24) term enrichment and Kyoto Encyclopedia of Genes and Genomes (KEGG) (24) pathway analysis, were conducted by means of clusterProfiler (version 3.2.11, http://www.bioconductor.org/packages/release/bioc/html/clusterProfiler.html) (25) in R package. A $p < 0.05$ and count ≥ 2 was considered the threshold value.

Analysis of immune-related DEGs in T cells

By applying CIBERSORT (26), the abundance of six types of infiltrating immune cells, including $CD4^+$ T cells, $CD8^+$ T cells, B cells, macrophages, neutrophils, and dendritic cells, was calculated. Twenty-two functionally defined human immune subsets (LM22) were used as a reference expression signature. The histogram for displaying the abundance of immune cell infiltration in the samples was then generated using the ggplot2 package (version: 3.2.1) in R package. The Pearson correlation coefficient between DEGs and the abundance of $CD4^+$ or $CD8^+$ T cells was analyzed, followed by the analysis of their immune-related DEGs with a threshold value of $|r| > 0.2$.

PPI network construction

The interactions between immune-related DEGs of T cells were retrieved based on the information on the STRING (version: 10.0, http://string-db.org/) (27) database with a combined score of 0.4. The PPI network was visualized using Cytoscape (version: 3.2.0, http://www.cytoscape.org/) (28).

The construction of the miRNA-target regulatory network

The miRNAs targeting immune-related DEGs of T cells were predicted using miRWalk 3.0 (http://zmf.umm.uni-heidelberg.de/apps/zmf/mirwalk3.html) (29) with score > 0.95. Moreover, the

miRNA-target interactions that existed in the two of the following databases, i.e., TargetScan (http://www.targetscan.org/), miRDB (http://www.mirdb.org/miRDB/download.html), and mirtarbase release 7.0 (http://mirtarbase.mbc.nctu.edu.tw), were selected for miRNA-target regulatory network construction.

Construction of the ceRNA network

The lncRNAs that could interact with the miRNAs in the miRNA-target regulatory network were predicted using the Prediction Module (score = 1) in DIANA-LncBase v.2 (http://carolina.imis.athena-innovation.gr/diana_tools/web/index.php?r=lncbasev2%2Findex) (30), and the lncRNA-miRNA interactions were obtained. By the integration of lncRNA-miRNA and miRNA-target interactions, the ceRNA (lncRNA-miRNA-target) network was constructed.

Construction of thechemical small molecule-target network

Using Ovarian Neoplasms (Synonym: Ovarian Cancer) as the keyword, disease-related molecules were analyzed using the Comparative Toxicogenomics Database (CTD, http://ctd.mdibl.org/) (31). By comparing the results with those obtained from the ceRNA network, the chemical small molecule-target interactions were obtained, and its related network was constructed using Cytoscape.

Survival analysis of immune-related DEGs in T cells

The prognosis-related clinical data in TCGA were retrieved, including overall survival (OS) and OS status. Based on the median expression value, the immune-related DEGs in T cells were divided into high and low expression groups. Subsequently, Kaplan-Meier (K-M) survival curves were plotted together with a log-rank statistical test. $p < 0.05$ was set as the significant threshold value to select prognosis-related genes.

Results

DEGs were screened based on immune score and stromal score groups

In total, 723 DEGs (63 upregulated and 610 downregulated) and 751 DEGs (113 upregulated and 688 downregulated) were screened in high immune score and stromal score groups, in comparison to those in low immune and stromal score groups, respectively.

Function analysis for DEGs

The results of the functional enrichment analysis revealed that the upregulated intersection genes were significantly enriched in 46 GO BP terms but were not enriched in any KEGG pathway. The downregulated intersection genes were significantly enriched in 935 GO BP terms and 56 KEGG pathways. The top 20 enriched GO terms or KEGG pathways are shown in Supplemental Fig. 2.

Analysis of immune-related DEGs associated with tumor-infiltrating T cells

The abundance of six types of infiltrating immune cells, including $CD4^+$ and $CD8^+$ T cells, was calculated by CIBERSORT, and the histogram of the abundance of immune cell infiltration in the samples are shown in Fig. 1. By Pearson correlation analyses, 37 and 49 immune-related DEGs of $CD4^+$ and $CD8^+$ T cells, respectively, were obtained. Notably, these immune-related genes were all downregulated.

Interaction analyses between immune-related DEGs in T cells based on PPI network

The PPI network constructed by immune-related DEGs in $CD4^+$ T cells consisted of 36 nodes and 219 interaction relation pairs (Fig. 2A). The PPI network constructed by immune-related DEGs in $CD8^+$ T cells contained 46 nodes and 331 interaction relation pairs (Fig. 2B). Interestingly, granzyme B (GZMB) was identified as the hub node in two PPI networks with the highest degree.

Prediction of immune-related miRNAs based on miRNA-target regulatory network

In total, 18 miRNAs that could target six immune-related DEGs of $CD4^+$ T cells were predicted, and 18 miRNA-target pairs were obtained. The miRNA-target regulatory network of $CD4^+$ T cells is shown in Fig. 3A. The apolipoprotein L6 (APOL6) was targeted by the greatest number of miRNAs in this network, such as has-miR-6867-5p. In addition, 12 miRNAs that could target five immune-related DEGs of CD8 + T cells were predicted, and 12 miRNA-target pairs were obtained. The miRNA-target regulatory network of $CD8^+$ T cells is shown in Fig. 3B. CD3E was targeted by the greatest number of miRNAs, such as has-miR-1249-5p.

Analysis of the immune-related ceRNA network in T cells

Using the DIANA-LncBase v2, 45 lncRNAs that could interact with 16 miRNAs in the miRNA-target regulatory network of $CD4^+$ T cells were obtained. From these, chr22-38_28785274-29006793.1 could interact with the greatest number of miRNAs. By the integration of lncRNA-miRNA and miRNA-target interactions, the ceRNA network in $CD4^+$ T cells (which included 45 lncRNA, 16 miRNAs, 6 immune-related DEGs in $CD4^+$ T cells, and 79 ceRNA interactions) was constructed (Fig. 3C). Moreover, 9 lncRNAs that could interact with 11 miRNAs in the miRNA-target regulatory network of $CD8^+$ T cells were predicted, and chr22-38_28785274-29006793.1 could also interact with the greatest number of miRNAs. By the integration of lncRNA-miRNA and miRNA-target interactions, the ceRNA network of $CD8^+$ T cells (which included 9 lncRNA, 11 miRNAs, 5 immune-related DEGs in $CD8^+$ T cells, and 31 ceRNA interactions) was constructed (Fig. 3D). Intriguingly, chr22-38_28785274-29006793.1/has-miR-1249-5p/CD3E was obtained from both ceRNA networks.

Screening chemical small molecules associated with tumor-infiltrating T cells

Based on the information of the CTD, 90 chemical small molecule-target pairs in $CD4^+$ T cells were obtained. There were three lncRNAs, five immune-related DEGs, and 43 chemical small molecules in the small molecule-target network of $CD4^+$ T cells (Fig. 4A). In addition, 86 chemical small molecule-target pairs in $CD8^+$ T cells were obtained. There was one lncRNA, four immune-related DEGs, and 42 chemical small molecules in the small-molecule target network of $CD8^+$ T cells (Fig. 4B). Notably, CD3E was found to be targeted by 14 chemical small molecules, including 1,3-butadiene, arsenic, benzene, benzo(a)pyrene, bisphenol A, cyclophosphamide, dexamethasone, diethylstilbestrol, estradiol, (+)-JQ1 compound, progesterone, resveratrol, tetrachlorodibenzodioxin, and topotecan.

GZMB and CD3E were correlated with the survival of OV patients

Survival analyses were performed to analyze prognosis-related genes. The results showed that 19 and 19 immune-related DEGs of $CD4^+$ and $CD8^+$ T cells, which all included GZMB and CD3E, had a significant positive correlation with OS of OV patients (Fig. 5). GZMB and CD3E were common immune-related DEGs associated with both $CD4^+$ and $CD8^+$ T cells.

Discussion

OV is one of the most common oncogenic malignancies among women. Despite multiple progress in OV treatment, 70–80% of patients with OV who initially respond to treatment eventually relapse and die (32). Immunotherapy as a cancer treatment has become a growing field, but reports of success in treating epithelial OV are limited (33). Tumor-infiltrating T cells in the tumor microenvironment are reported to be the biological basis of immunotherapy and promising predictors of cancer prognosis (14). Therefore, investigation of immune-related RNAs associated with tumor-infiltrating T cells in OV patients could be helpful in finding prognostic markers for OV.

In the present study, we calculated the immune and stromal scores on the basis of gene expression data of patients with OV, and the immune-related DEGs associated with tumor-infiltrating T cells were analyzed. The results showed that 37 and 49 immune-related DEGs of $CD4^+$ and $CD8^+$ T cells, respectively, were screened. Subsequently, the PPI network showed that GZMB was a hub node in both PPI networks constructed by immune-related DEGs of $CD4^+$ and $CD8^+$ T cells. Moreover, the ceRNA chr22-38_28785274-29006793.1/ has-miR-1249-5p/CD3E was obtained from the constructed ceRNA networks associated with $CD4^+$ and $CD8^+$ T cells. Furthermore, survival analysis results revealed that key immune-related DEGs of $CD4^+$ and $CD8^+$ T cells, such as GZMB and CD3E, were positively correlated with patient prognosis. These results merit further discussion.

GZMB is a serine protease that is primarily expressed by multiple immune cells, including macrophages, lymphocytes, and mast cells (34). It is reported that GZMB is used by activated cytotoxic T lymphocytes to induce apoptosis of target cells (35). In tumor-infiltrating cytotoxic T lymphocytes, type I interferon is

found to inhibit tumor growth by inducing STAT3 activation to promote the expression of GZMB (36). Moreover, Prizment et al. has demonstrated that GZMB expression is correlated with the improved survival of patients with colorectal cancer and might be used as a useful prognostic factor (37). In our study, GZMB was a hub node in the two PPI networks constructed by immune-related DEGs of $CD4^+$ and $CD8^+$ T cells. Moreover, GZMB was found to be positively correlated with patient prognosis. Thus, we speculate that GZMB could be used as a potential prognostic marker of tumor-infiltrating T cells for OV.

CD3E is one of the four invariant chains physically associated with the T-cell receptor (TCR), and the TCR–CD3 complex has been reported to exert a significant function in the immune system (38). The combined immunoscore of CD103 and CD3 may be used to identify patients with early relapse or long-term survival in serous OV (39). We found that CD3E was targeted by the greatest number of miRNAs in the miRNA-target regulatory network, and CD3E showed significant positive correlation with patient OS. Therefore, CD3E may also be a promising prognostic marker of tumor-infiltrating T cells for OV. In addition, CD3E was found to be targeted by several chemical small molecules, such as 1,3-butadiene and benzene. It is reported that 1,3-butadiene and benzene exposure can increase lifetime risk of cancer (40). Thus, we speculate that monitoring the expression of CD3E could be used to predict lifetime risk of cancer caused by exposure to chemical small molecules.

Furthermore, miRNAs able to target CD3 subunit molecules and affect the immune system are considered as promising biomarkers for early cancer detection (41). In our study, we found that CD3E was targeted by multiple miRNAs, such as has-miR-1249-5p. miR-1249 is found to act as either an oncogene or tumor suppressor in different tumor types. For instance, miR-1249 is upregulated in patients with small cell carcinoma of the esophagus, and its enhanced expression is associated with tumor relapse (42). Nevertheless, miR-1249 is shown to be markedly downregulated in colorectal cancer tissues, and it may serve as a novel therapeutic target (43). Our data predicted the target relationship between miR-1249-5p and CD3E. Although little is known about miR-1249 in OV, our result prompts us to speculate that miR-1249-5p may be a potential regulator mediating the key role of tumor-infiltrating T lymphocytes in OV via the targeting of CD3E. In addition, existing evidence has confirmed that lncRNAs function as ceRNAs to competitively bind to the miRNA binding sites, consequently reducing their regulatory effect on target mRNAs (44, 45). Our results showed that the ceRNA chr22-38_28785274-29006793.1/has-miR-1249-5p/CD3E was obtained from the two constructed ceRNA networks related to $CD4^+$ and $CD8^+$ T cells. Therefore, we speculate that ceRNAs, such as chr22-38_28785274-29006793.1/has-miR-1249-5p/CD3E, could be a target of tumor-infiltrating T cells and are involved in the immune escape of tumors in OV. It would be interesting to further investigate the clinical significance of ceRNA chr22-38_28785274-29006793.1/has-miR-1249-5p/CD3E in OV.

In conclusion, our data reveal that tumor-infiltrating T cells may contribute to the immune escape of tumor cells in OV by regulating GZMB and ceRNAs, such as chr22-38_28785274-29006793.1/has-miR-1249-5p/CD3E. GZMB and CD3E may serve as promising T cell immune-related biomarkers with prognostic value in OV.

Declarations

Ethics approval and consent to participate

NA

Competing Interests

he authors declare that no conflicts of interest exist.

Authors' Contributions

All authors participated in the conception and design of the study.

Conceived and drafted the manuscript: Liao Haihong and Han Shuwen;
Collated and proofread the literature: Pan Yuefen, Xu Jiamin, Qi Quan;

Wrote the paper: Jiang Yizhen and Yang Xi;
All authors read and approved the paper.

Founding

This work was supported by the Zhejiang Medical and Health Technology Projects (No. 2019RC285).

Competing Interests

The authors declare that no conflicts of interest exist.

Data Availability Statement

Data is available by contacting the corresponding author.

References

1. Momenimovahed Z, Tiznobaik A, Taheri S, Salehiniya H. Ovarian cancer in the world: epidemiology and risk factors. International journal of women's health. 2019;11:287.
2. Bray F, Ferlay J, Soerjomataram I, Siegel RL, Torre LA, Jemal A. Global cancer statistics 2018: GLOBOCAN estimates of incidence and mortality worldwide for 36 cancers in 185 countries. Cancer J Clin. 2018;68(6):394–424.

3. Travers M, Brown SM, Dunworth M, Holbert CE, Wiehagen KR, Bachman KE, et al. DFMO and 5-azacytidine increase M1 macrophages in the tumor microenvironment of murine ovarian cancer. Cancer research. 2019;79(13):3445–54.
4. Jacobs IJ, Menon U, Ryan A, Gentry-Maharaj A, Burnell M, Kalsi JK, et al. Ovarian cancer screening and mortality in the UK Collaborative Trial of Ovarian Cancer Screening (UKCTOCS): a randomised controlled trial. The Lancet. 2016;387(10022):945–56.
5. Jacob F, Nixdorf S, Hacker NF, Heinzelmannschwarz VA. Reliable in vitro studies require appropriate ovarian cancer cell lines. Journal of Ovarian Research. 2014;7(1):60.
6. Pardoll DM. The blockade of immune checkpoints in cancer immunotherapy. Nat Rev Cancer. 2012;12(4):252–64.
7. Sharma P, Wagner K, Wolchok JD, Allison JP. Novel cancer immunotherapy agents with survival benefit: recent successes and next steps. Nat Rev Cancer. 2011;11(11):805–12.
8. Binnewies M, Roberts EW, Kersten K, Chan V, Fearon DF, Merad M, et al. Understanding the tumor immune microenvironment (TIME) for effective therapy. Nature medicine. 2018;24(5):541–50.
9. Zhang L, Conejo-Garcia JR, Katsaros D, Gimotty PA, Massobrio M, Regnani G, et al. Intratumoral T cells, recurrence, and survival in epithelial ovarian cancer. N Engl J Med. 2003;348(3):203–13.
10. Loi S, Drubay D, Adams S, Pruneri G, Francis PA, Lacroix-Triki M, et al. Tumor-infiltrating lymphocytes and prognosis: a pooled individual patient analysis of early-stage triple-negative breast cancers. Journal of clinical oncology. 2019;37(7):559.
11. Bremnes RM, Busund L-T, Kilvær TL, Andersen S, Richardsen E, Paulsen EE, et al. The role of tumor-infiltrating lymphocytes in development, progression, and prognosis of non–small cell lung cancer. Journal of Thoracic Oncology. 2016;11(6):789–800.
12. Peled M, Onn A, Herbst RS. Tumor-infiltrating lymphocytes—location for prognostic evaluation. Clin Cancer Res. 2019;25(5):1449–51.
13. Balatoni T, Mohos A, Papp E, Sebestyén T, Liszkay G, Oláh J, et al. Tumor-infiltrating immune cells as potential biomarkers predicting response to treatment and survival in patients with metastatic melanoma receiving ipilimumab therapy. Cancer Immunol Immunother. 2018;67(1):141–51.
14. Wang W, Zou W, Liu JR. Tumor-infiltrating T cells in epithelial ovarian cancer: predictors of prognosis and biological basis of immunotherapy. Gynecol Oncol. 2018;151(1):1–3.
15. Nielsen JS, Sahota RA, Milne K, Kost SE, Nesslinger NJ, Watson PH, et al. CD20 + tumor-infiltrating lymphocytes have an atypical CD27- memory phenotype and together with CD8 + T cells promote favorable prognosis in ovarian cancer. Clin Cancer Res. 2012;18(12):3281–92.
16. Di Jia SL, Li D, Xue H, Yang D, Liu Y. Mining TCGA database for genes of prognostic value in glioblastoma microenvironment. Aging. 2018;10(4):592.
17. Romero-Garcia S, Moreno-Altamirano MMB, Prado-Garcia H, Sánchez-García FJ. Lactate contribution to the tumor microenvironment: mechanisms, effects on immune cells and therapeutic relevance. Frontiers in immunology. 2016;7:52.

18. Lambrechts D, Wauters E, Boeckx B, Aibar S, Nittner D, Burton O, et al. Phenotype molding of stromal cells in the lung tumor microenvironment. Nature medicine. 2018;24(8):1277–89.
19. Zeng Q, Zhang W, Li X, Lai J, Li Z. Bioinformatic identification of renal cell carcinoma microenvironment-associated biomarkers with therapeutic and prognostic value. Life Sci. 2020;243:117273.
20. Yang S, Liu T, Nan H, Wang Y, Chen H, Zhang X, et al. Comprehensive analysis of prognostic immune-related genes in the tumor microenvironment of cutaneous melanoma. Journal of cellular physiology. 2020;235(2):1025–35.
21. Yoshihara K, Shahmoradgoli M, Martínez E, Vegesna R, Kim H, Torres-Garcia W, et al. Inferring tumour purity and stromal and immune cell admixture from expression data. Nature communications. 2013;4(1):2612.
22. Smyth GK. limma: Linear Models for Microarray Data. In: Gentleman R, Carey VJ, Huber W, Irizarry RA, Dudoit S, editors. Bioinformatics and Computational Biology Solutions Using R and Bioconductor. New York: Springer New York; 2005. pp. 397–420.
23. Benjamini Y, Hochberg Y. Controlling the false discovery rate: a practical and powerful approach to multiple testing. Journal of the Royal Statistical Society Series B (Methodological). 1995:289–300.
24. Kanehisa M, Goto S. KEGG: Kyoto Encyclopedia of Genes and Genomes. Nucleic Acids Res. 2000;28(1):27–30.
25. Yu G, Wang L, Han Y, He Q. clusterProfiler: an R package for comparing biological themes among gene clusters. OMICS. 2012;16(5):284–7.
26. Newman AM, Liu CL, Green MR, Gentles AJ, Feng W, Xu Y, et al. Robust enumeration of cell subsets from tissue expression profiles. Nat Methods. 2015;12:453.
27. Szklarczyk D, Franceschini A, Wyder S, Forslund K, Heller D, Huerta-Cepas J, et al. STRING v10: protein–protein interaction networks, integrated over the tree of life. Nucleic acids research. 2014:gku1003.
28. Shannon P, Markiel A, Ozier O, Baliga NS, Wang JT, Ramage D, et al. Cytoscape: A Software Environment for Integrated Models of Biomolecular Interaction Networks. Genome Res. 2003;13(11):2498–504.
29. Dweep H, Gretz N. miRWalk2.0: a comprehensive atlas of microRNA-target interactions. Nat Methods. 2015;12(8):697.
30. Paraskevopoulou M, Vlachos I, Karagkouni D, Georgakilas G, Kanellos I, Vergoulis T, et al. DIANA-LncBase v2: indexing microRNA targets on non-coding transcripts. Nucleic Acids Res. 2016;44(D1):D231-8.
31. Davis AP, Grondin CJ, Johnson RJ, Sciaky D, McMorran R, Wiegers J, et al. The Comparative Toxicogenomics Database: update 2019. Nucleic acids research. 2018:gky868-gky.
32. Varas-Godoy M, Rice G, Illanes SE. The crosstalk between ovarian cancer stem cell niche and the tumor microenvironment. Stem Cells International. 2017;2017.

33. Rodriguez GM, Galpin KJ, McCloskey CW, Vanderhyden BC. The tumor microenvironment of epithelial ovarian cancer and its influence on response to immunotherapy. Cancers. 2018;10(8):242.
34. Hendel A, Hiebert P, Boivin W, Williams S, Granville D. Granzymes in age-related cardiovascular and pulmonary diseases. Cell Death Differentiation. 2010;17(4):596–606.
35. Thomas DA, Scorrano L, Putcha GV, Korsmeyer SJ, Ley TJ. Granzyme B can cause mitochondrial depolarization and cell death in the absence of BID, BAX, and BAK. Proceedings of the National Academy of Sciences. 2001;98(26):14985-90.
36. Lu C, Klement JD, Ibrahim ML, Xiao W, Redd PS, Nayak-Kapoor A, et al. Type I interferon suppresses tumor growth through activating the STAT3-granzyme B pathway in tumor-infiltrating cytotoxic T lymphocytes. J immunother Cancer. 2019;7(1):157.
37. Prizment AE, Vierkant RA, Smyrk TC, Tillmans LS, Nelson HH, Lynch CF, et al. Cytotoxic T cells and granzyme B associated with improved colorectal cancer survival in a prospective cohort of older women. Cancer Epidemiology Prevention Biomarkers. 2017;26(4):622–31.
38. Call ME, Pyrdol J, Wucherpfennig KW. Stoichiometry of the T-cell receptor–CD3 complex and key intermediates assembled in the endoplasmic reticulum. EMBO J. 2004;23(12):2348–57.
39. Bösmüller H-C, Wagner P, Peper JK, Schuster H, Pham DL, Greif K, et al. Combined immunoscore of CD103 and CD3 identifies long-term survivors in high-grade serous ovarian cancer. International Journal of Gynecologic Cancer. 2016;26(4):671–9.
40. Thongkum W, Wibuloutai J, Thitisutthi S. Benzene and 1, 3 Butadiene Concentration and Its Potential Health Impact in Chiang Mai, Thailand. European Journal of Sustainable Development. 2017;6(2):187-.
41. Alashti FA, Minuchehr Z. MiRNAs which target CD3 subunits could be potential biomarkers for cancers. PloS one. 2013;8(11).
42. Okumura T, Shimada Y, Omura T, Hirano K, Nagata T, Tsukada K. MicroRNA profiles to predict postoperative prognosis in patients with small cell carcinoma of the esophagus. Anticancer research. 2015;35(2):719–27.
43. Chen X, Zeng K, Xu M, Liu X, Hu X, Xu T, et al. P53-induced miR-1249 inhibits tumor growth, metastasis, and angiogenesis by targeting VEGFA and HMGA2. Cell death disease. 2019;10(2):1–15.
44. Karreth FA, Pandolfi PP. ceRNA cross-talk in cancer: when ce-bling rivalries go awry. Cancer discovery. 2013;3(10):1113–21.
45. Salmena L, Poliseno L, Tay Y, Kats L, Pandolfi P. A ceRNA hypothesis: the Rosetta Stone of a hidden RNA language? Cell 2011; 146: 353–358. Cell Physiol Biochem. 2018;50:108 – 20.

Figures

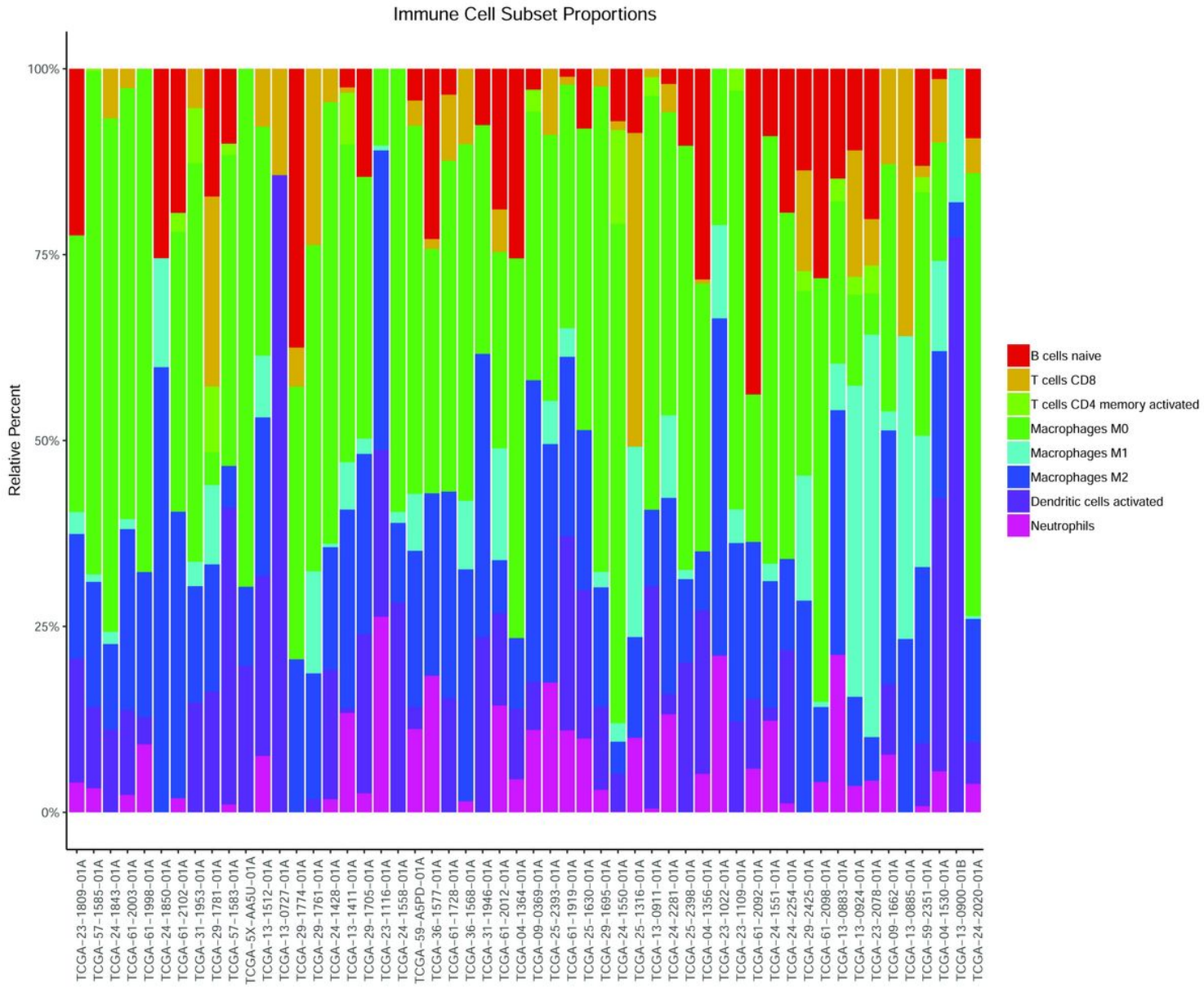

Figure 1

The histogram of immune cell infiltration in the tumor samples. Bar charts indicate the infiltration abundance of different immune cells. The abscissa axis represents the sample name. The longitudinal axis represents the relative percent of different types of infiltrating immune cells. Different colors indicate different types of infiltrating immune cells.

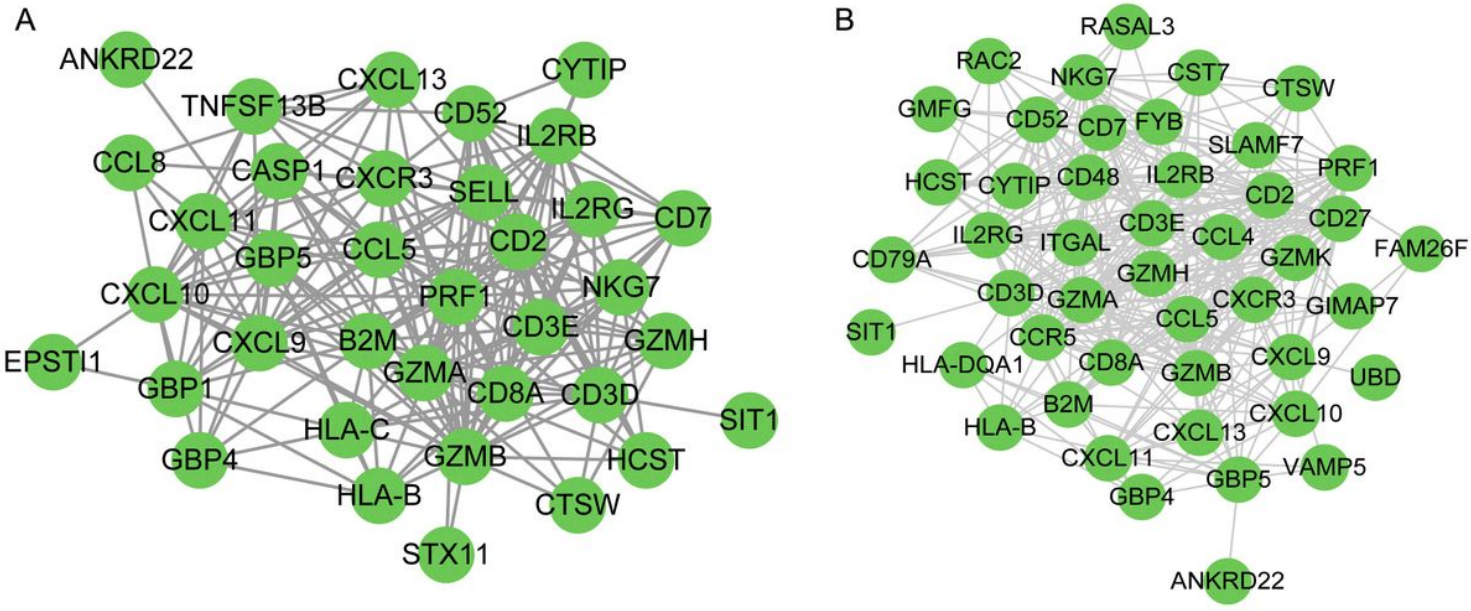

Figure 2

T cells immune-related protein-protein interaction (PPI) networks. A: PPI network constructed by immune-related DEGs of CD4+ T cells. B: PPI network constructed by immune-related DEGs of CD8+ T cells. All green nodes were downregulated genes in the two PPI networks. The lines stand for the interaction between nodes.

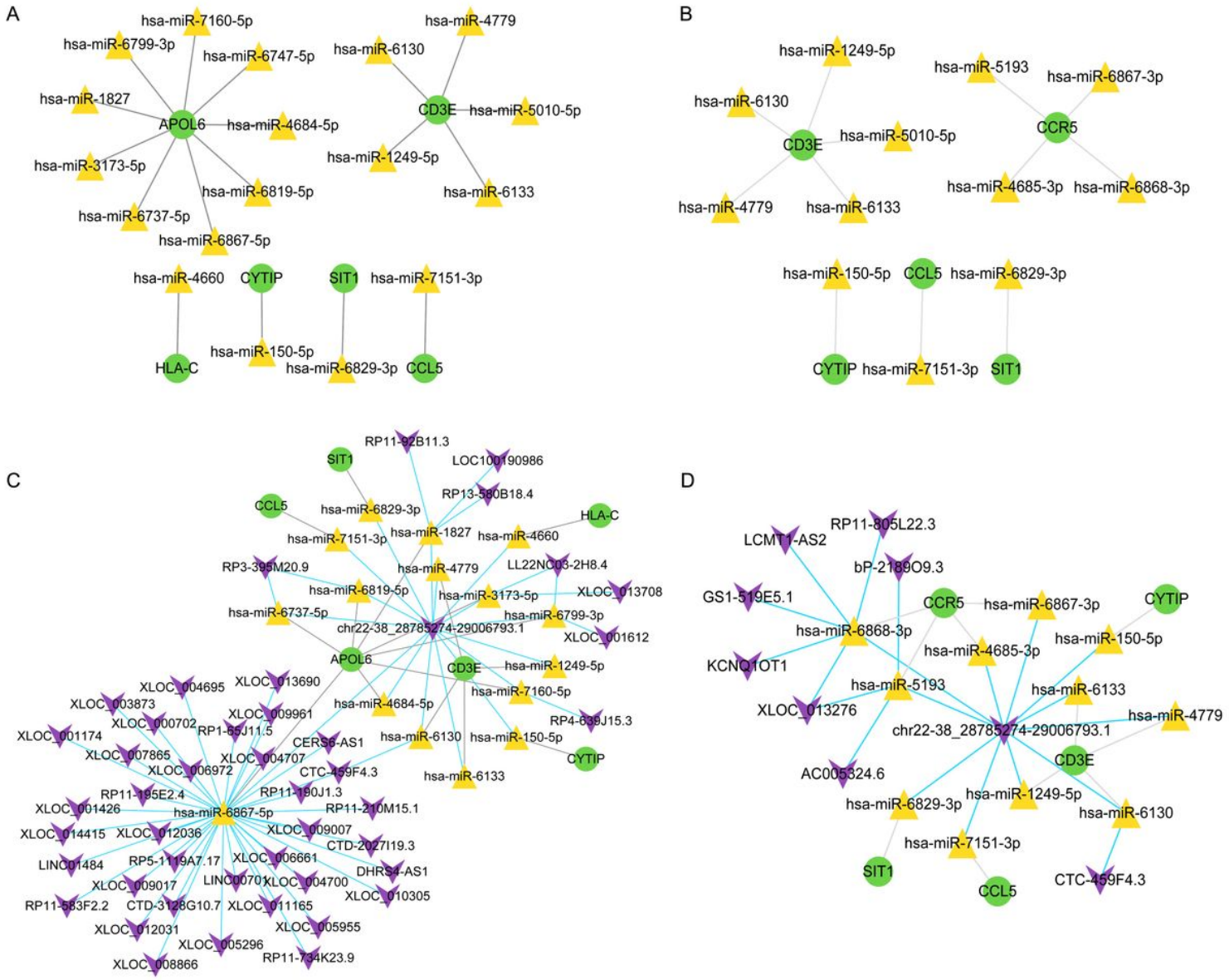

Figure 3

Immune-related miRNA-target regulatory networks and ceRNA networks of T cells. A: The immune-related miRNA-target regulatory network of CD4+ T cells. B: The immune-related miRNA-target regulatory network of CD8+ T cells. C: The immune-related ceRNA network of CD4+ T cells. D: The immune-related ceRNA network of CD8+ T cells. Green circular nodes are downregulated mRNAs, yellow triangle nodes are miRNAs, and purple and inverted triangle nodes are lncRNAs. The grey lines stand for the interaction between miRNAs and mRNAs. The blue lines stand for the interaction between miRNAs and lncRNAs.

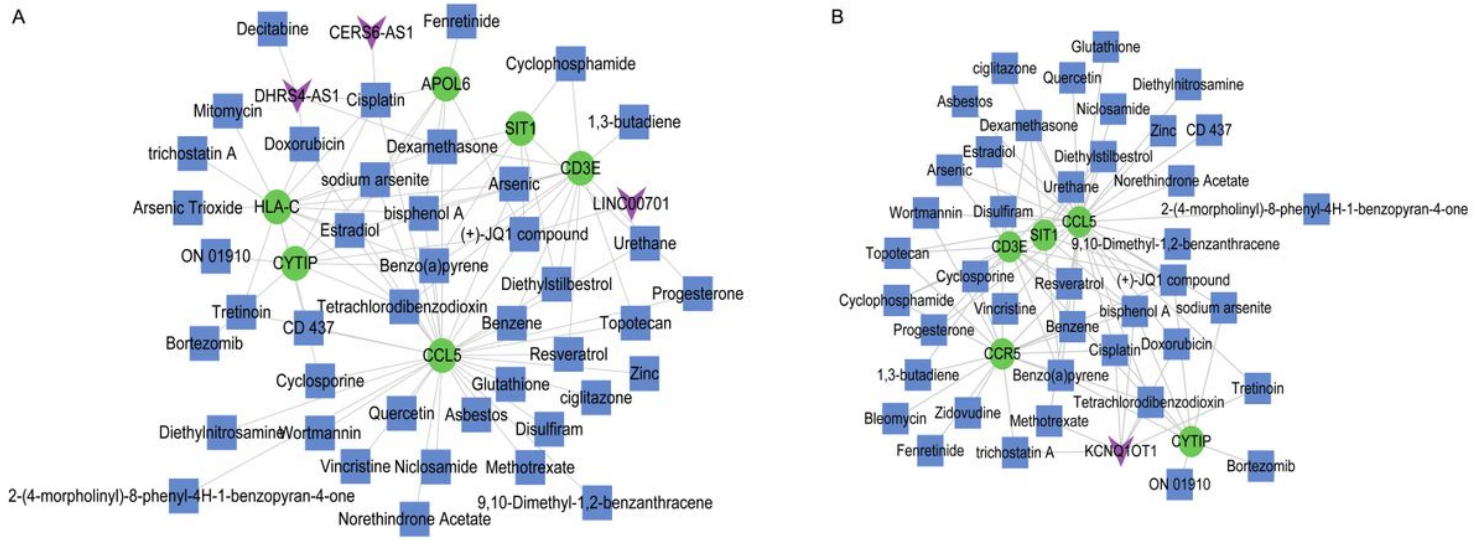

Figure 4

Immune-related chemical small molecule-target networks of T cells. A: The immune-related chemical small molecule-target network of CD4+ T cells. B: The immune-related chemical small molecule-target network of CD8+ T cells. Green circular nodes are downregulated mRNAs, blue square nodes are small molecules, and purple and inverted triangle nodes are lncRNAs. The lines stand for the interaction between nodes.

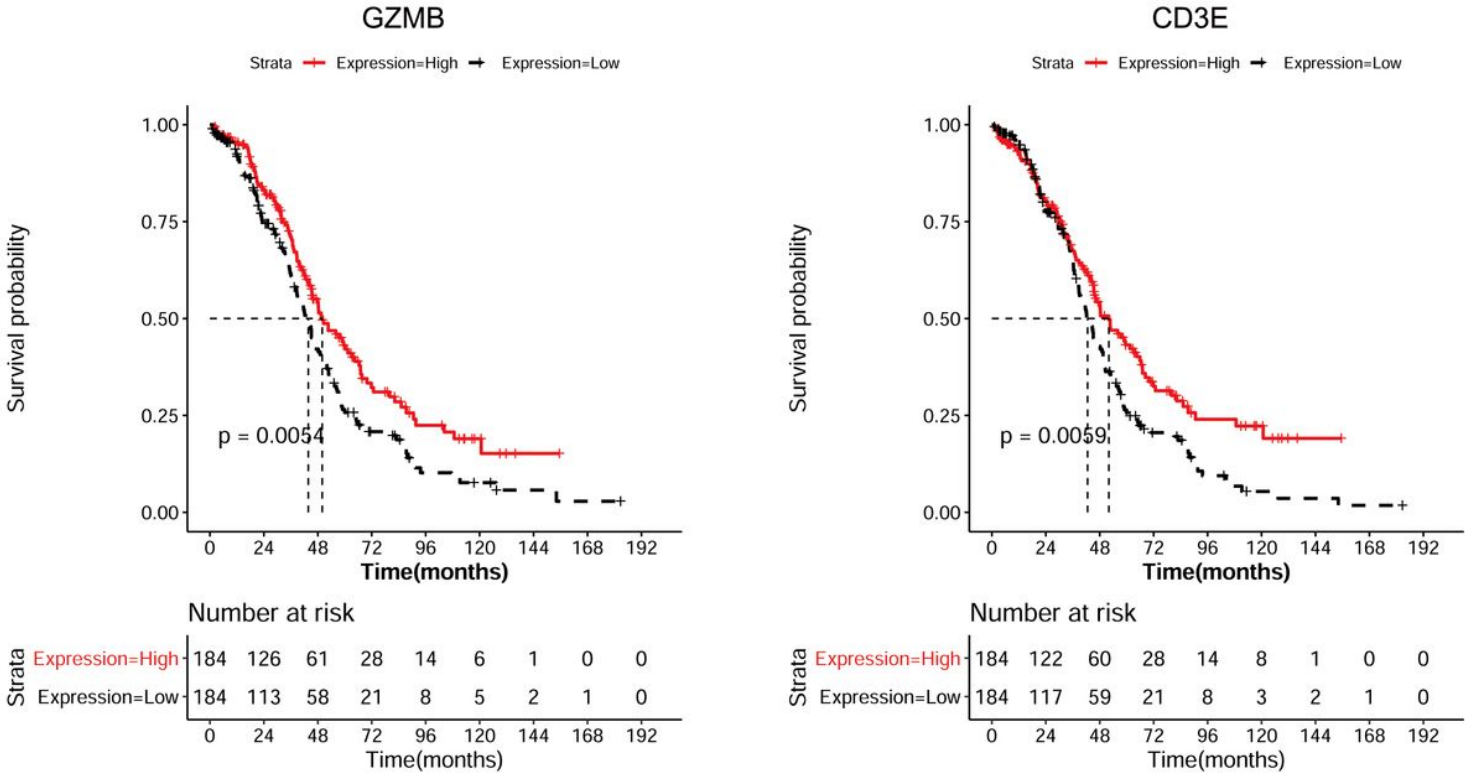

Figure 5

The prognostic value of GZMB and CD3E in patients with OA (Kaplan-Meier plotter). The abscissa axis is the survival time (months), and the longitudinal axis is the overall survival. The p-value was calculated using the log-rank statistical test.

Supplementary Files

This is a list of supplementary files associated with this preprint. Click to download.

- Highlight.doc
- SupplementalFigure2.tif
- SupplementalFigure1.tif